Available online at www.sciencedirect.com
ScienceDirect
Applied Thermal Engineering 28 (2008) 1774–1781
APPLIED THERMAL ENGINEERING
www.elsevier.com/locate/apthermeng

Application of aluminum oxide nanofluids in diesel electric generator as jacket water coolant

Devdatta P. Kulkarni, Ravikanth S. Vajjha, Debendra K. Das *, Daniel Oliva

Department of Mechanical Engineering, University of Alaska Fairbanks, P.O. Box 755905, Fairbanks, AK 99775-5905, USA

Received 22 April 2007; accepted 12 November 2007
Available online 30 June 2008

Abstract

This paper presents a study on nanofluids applications, such as a coolant in a diesel electric generator (DEG). Specific heat measurements of aluminum oxide nanofluid with various particle concentrations have been presented demonstrating a reduction in their values with an increase in the particle concentration and an increase with temperature. Experiments were performed on the DEG to assess the effect of nanofluids on cogeneration efficiency. The investigation showed that applying nanofluids resulted in a reduction of cogeneration efficiency. This is due to the decrease in specific heat, which influences the waste heat recovery from the engine. However, it was found that the efficiency of waste heat recovery heat exchanger increased for nanofluid, due to its superior convective heat transfer coefficient.

Keywords: Nanofluids; Specific heat; Cogeneration; Efficiency; Diesel electric generator

1. Introduction

Cooling is one of the most important technical challenges facing numerous industries such as automobiles, electronics and manufacturing. New technological developments are increasing thermal loads and requiring faster cooling. The conventional methods in increasing the cooling rate (fins and microchannels) are already stretched to their limits. Hence, there is an urgent need for new and innovative coolants to achieve this high performance cooling [1,2]. Thermal conductivities of traditional heat transfer fluids, such as engine coolants, lubricants and water are very low. With increasing global competition, industries have a strong need to develop energy efficient heat transfer fluids with significantly higher thermal conductivities than the available fluids. Also, government agencies like the Environmental Protection Agency are imposing more stringent criteria for pollution and automobile emissions. The new coolants with their higher thermal performance will reduce the overall size of heat exchanger/radiator and may decrease vehicle fuel consumption.

Nanofluids are a novel concept. They are heat transfer fluids containing suspended nanoparticles, which have been developed to meet more demanding cooling challenges. Nanofluids are a new class of solid–liquid composites consisting of nanometer sized (<100 nm) solid particles suspended in heat transfer fluids such as water, ethylene and propylene glycol. The improvement of lubricity by adding nanoparticles to engine oil is under investigation [3].

Choi et al. [4] showed that nanofluids have the potential to be the next generation of coolants for vehicle thermal management due to their significantly higher thermal conductivities. Several researchers [5–9] showed that the convective heat transfer coefficient increases substantially for nanofluids. The heat rejection requirements of automobiles and trucks are continually increasing due to trends toward more powerful outputs.

Heat transfer directly affects engine performance, fuel efficiency, materials selection and emissions. Managing the heat generated during combustion is particularly important in improving engine life, oil cooling and climate control. For electric and hybrid vehicles, thermal manage-

* Corresponding author. Tel.: +1 907 474 6094; fax: +1 907 474 6141.
E-mail address: ffdkd@uaf.edu (D.K. Das).

1359-4311/$ - see front matter © 2008 Published by Elsevier Ltd.
doi:10.1016/j.applthermaleng.2007.11.017

Nomenclature

C_p	specific heat, J/kg K
H_v	heating value of fuel, kJ/m^3 or Btu/gal
m	mass of fluid, kg
$\dot{m}$	mass flow rate, kg/s
Q_s	heat supplied, J
$\dot{Q}$	rate of heat supplied to fluid, W
$\dot{Q}_H$	rate of heat supplied by fuel, W
$\dot{Q}_{JW}$	rate of heat transported by jacket water, W
$\dot{Q}_{SW}$	rate of heat transported by shop water, W
T	temperature, °C
t	time, s
$\dot{V}$	volumetric flow rate, m^3/s
$\dot{V}_f$	volumetric flow rate of fuel, m^3/s
$\dot{W}_{el}$	electrical output, W

Greek symbols

ρ	density, kg/m^3
Δ	difference
η	efficiency
ϕ	volumetric concentration, %

Subscripts

cogen	cogeneration
el	electrical
f	fluid
in	into the engine for JW into the heat exchanger for SW
JW	jacket water
nf	nanofluid
out	out of the engine for JW out of the heat exchanger for SW
SW	shop water
s	solid

ment of advanced batteries will also be critically important. Improved thermal management systems for advanced vehicles require more compact heat exchangers, innovative heat transfer schemes and environmentally friendly fluids with improved heat transfer properties.

Nanofluids with improved properties could result in smaller, more efficient advanced vehicles. The benefits of improved heat exchangers and heat transfer devices using nanofluids are: reduced weight, which will improve fuel economy; smaller components, which take up less room under the hood and allow for greater latitude in aerodynamic styling; more effective cooling and increased component life. Additionally, mining efforts will be lower as less metal is required, minimizing the environmental impact and saving energy in metal production. By reducing the size, the solid waste disposal problem is diminished at the end of the useful life cycle of the heat transfer systems.

Utilizing nanofluids because of the benefits described above, this study focuses on evaluating the cogeneration and heat exchanger efficiency of a diesel generator with nanofluids as the coolant.

2. Experimental setup for specific heat measurement

Since specific heat contributes to faster and improved rates of heat transfer, accurate measurements are essential. The experimental setup for measuring the specific heat of the aluminum nanoparticles dispersed in 50:50 inhibited ethylene glycol and water (EG/W) mixture is shown in Fig. 1. The apparatus consists of a 7.6 cm (3 in.) ID and 22.9 cm (9 in.) long Acrylonitrile Butadieen Styrene (ABS) container, a low thermal conductivity material to minimize heat flow from the fluid into the container wall. The apparatus is designed to hold about one liter of liquid. Aluminum oxide nanofluids are heated from 25 °C to 70 °C by using an electrical immersion heater shown in Fig. 1. Four copper–constantan thermocouples are symmetrically placed at 1.9 cm (0.75 in.) radial distance from the center.

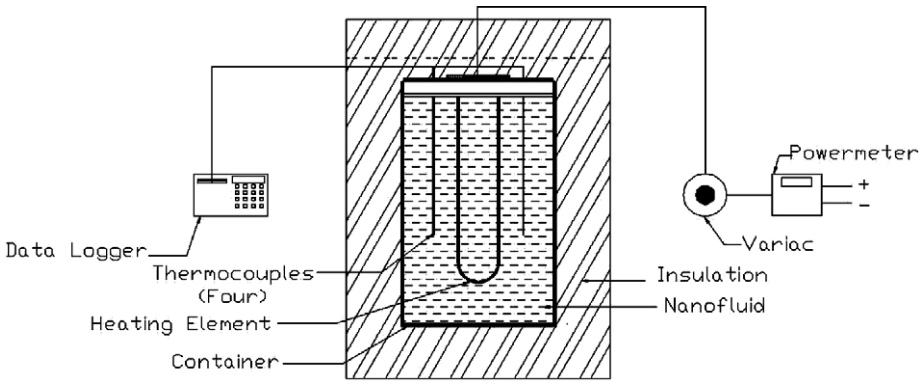

Fig. 1. Experimental setup for specific heat measurement of nanofluids.

The tips of thermocouple probes are at the mid-height of the container to monitor the temperature increase of the nanofluid. These thermocouples are connected to a data logger that records the temperature data at 5-s intervals. The container is insulated by two layers of insulation. The inner layer is 5.5 cm (2.125 in.) thick fiber glass insulation wrapped around the container. The outer layer consists of 10 cm (4 in.) thick extruded foam board insulation. This arrangement minimizes the heat flow away from the fluid. A variac is used to supply constant wattage to the immersion heater and the power input into the nanofluid is monitored by a power meter.

3. Benchmark test case for specific heat measurement

To verify the accuracy of the specific heat measurement apparatus and the experimental procedure, the specific heat of pure water was measured.

Deionized water of mass 1.05 kg at 25 °C was introduced into the container for the specific heat measurement. A constant heat rate of 35.5 W was supplied to the heating element to increase the temperature of water to 70 °C. The temperature change was recorded at every 5-s interval using thermocouples and data logger. The specific heat of water and each tested nanofluid was calculated from

$$C_{p\mathrm{nf}} = \frac{\dot{Q}}{m}\left(\frac{\Delta t}{\Delta T}\right) \tag{1}$$

The slope of the straight line in Fig. 2 is derived by plotting heat energy input Q_s (Joule) $= \dot{Q}\Delta t$ versus product of mass m (kg) and the temperature difference ΔT (Kelvin). This slope gives the specific heat of the fluid. Measurement of water temperatures at the top, middle and the bottom locations of the container showed that the middle thermocouples were giving a mean temperature of the fluid between the top and bottom layers. It was also observed that the slopes $(\Delta T/\Delta t)$ of temperature versus time plot for the top, middle and bottom layers of the fluid were parallel. As noticed from Eq. (1), $C_{p\mathrm{nf}}$ is a function of the slope $(\Delta T/\Delta t)$. This slope was nearly same for the top, middle and bottom locations. Therefore, the slope of the average temperatures of the middle four thermocouples was taken as an accurate approach to evaluate the specific heat $C_{p\mathrm{nf}}$. The obtained specific heat of the water was then compared to the value from American Society of Heating, Refrigerating and Air Conditioning Engineers (ASHRAE) handbook [10]. The experimental value at an average temperature of 50 °C only differed by ±0.2%, when compared with the ASHRAE value.

4. Discussion of specific heat results

After confirming the readings from the specific heat measurement apparatus with water, specific heat measurements for different volume concentrations of aluminum oxide nanofluid in 50:50 EG/W mixture were carried out.

The effective specific heat of nanofluids is given by Pak and Cho [11]

$$C_{p\mathrm{nf}} = (1-\phi)C_{p\mathrm{f}} + \phi C_{ps} \tag{2}$$

However, according to Buongiorno [12], the specific heat of a nanofluid should be calculated assuming the nanoparticles and base fluid are in thermal equilibrium. He presented the equation as

$$C_{p\mathrm{nf}} = \frac{\phi\rho_s C_{ps} + (1-\phi)\rho_f C_{p\mathrm{f}}}{\rho_{nf}} \tag{3}$$

Fig. 3 displays the specific heat variation for varying concentrations of aluminum oxide nanofluids. The experimental values are compared with the theoretical correlations presented in Pak and Cho [11] and Buongiorno [12]. It shows that Buongiorno's correlation is in better agreement than Pak and Cho's correlation with the experimental data. As the particle volume concentration increases, the specific heat of the aluminum nanofluids decreases. It implies for higher concentrations of aluminum nanofluid, less heat input is required to increase the temperature of the nanofluid,

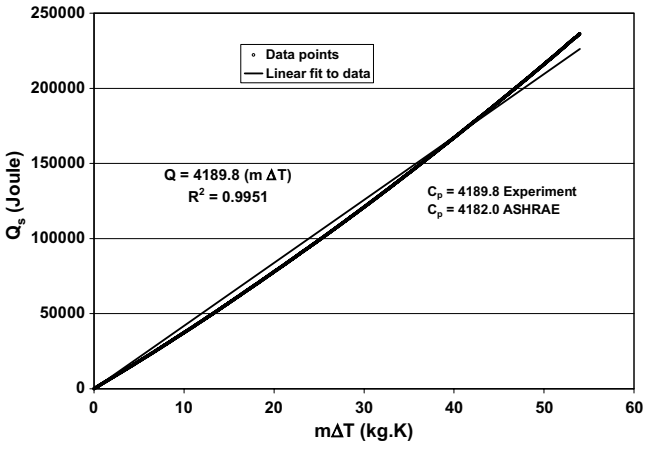

Fig. 2. Specific heat of water obtained from the experimental setup.

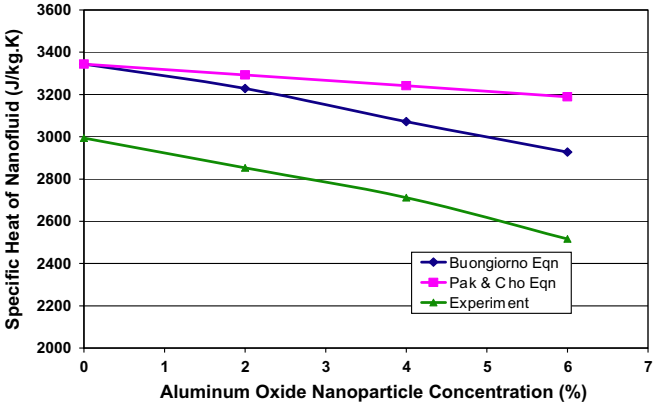

Fig. 3. Comparison of experimental and theoretical values of specific heat for aluminum oxide nanofluids at various concentrations suspended in 50:50 EG/W mixture at 25 °C.

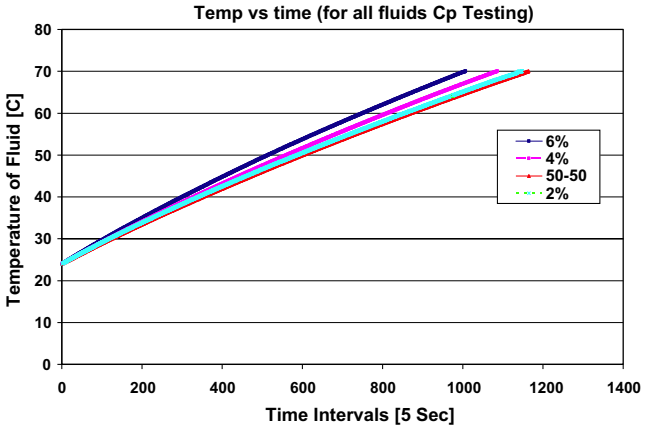

Fig. 4. Time versus temperature to heat aluminum nanofluids with varying concentrations in 50:50 ethylene glycol and water solution. The topmost curve is for 6% concentration and the lowest curve is for 50:50 EG/W.

or with the same heat input, the time required to reach 70 °C will diminish. The difference in the specific heat value (~7%) between experiment and from ASHRAE [10] at 0% concentration is due to the presence of the inhibitor in commercially available fluids.

The variation of temperature versus time for various volume concentrations of Al_2O_3 nanofluid at a constant heat input rate of 35.5 W is shown in Fig. 4. If the time required to heat reduces, this will be very beneficial in automobiles, especially in arctic or subarctic regions. By employing nanofluids as jacket water, the engine will heat up faster and may result in less emission to the environment, since higher concentration of pollutants are emitted during the engine warm-up.

5. Temperature dependent specific heat

From the experiments, it was determined that as the temperature of the nanofluid increased, the specific heat of the nanofluids also increased (Fig. 5). ASHRAE [10] also shows that the specific heat of glycol and water mixtures increases with temperature. This has a very profound impact. Most of the heat transfer fluids operate at a temperature greater than room temperature in heat exchangers. Therefore, there is a need to find the temperature dependency of the nanofluid specific heat. Until now, all the numerical and experimental analyses in various literatures [13–18], use a constant value of the specific heat at 20 °C. This must have introduced substantial errors in their results.

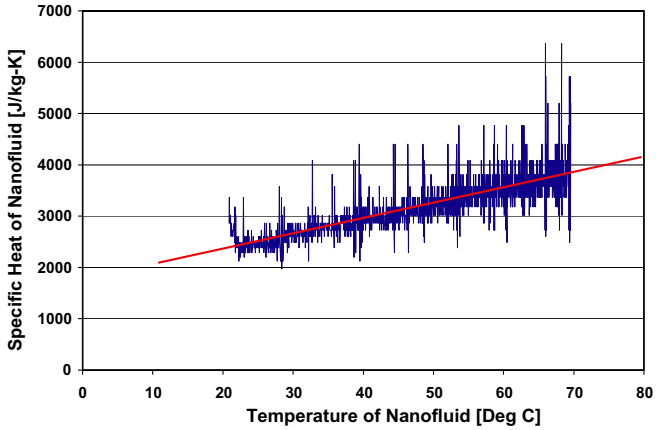

Fig. 5. Temperature dependent specific heat of 6% aluminum oxide in EG/W nanofluid.

6. Cogeneration efficiency

In the case of a diesel generator, the efficiency is defined by the ratio of the electrical power produced and the energy rate associated with the fuel input to the generator. However, this efficiency is quite low, often in the range of 25–38%, due to the large amount of waste heat in the system. A method to increase the overall efficiency of a diesel engine is to capture some of the escaping heat energy with a heat exchanger, and utilize that energy to produce a useful deliverable. Cogeneration efficiency η_{cogen}, is defined as follows:

$$\eta_{\text{cogen}} = (\text{Electrical Power} + \text{Rate of Heat Recovered})/\text{Fuel Consumption energy rate} \quad (4)$$

Cogeneration efficiency can be as high as 80%. This is a substantial and very useful increase in efficiency; especially in arctic regions where the heat energy is useful to heat buildings. In warmer climates the heat energy can be collected and used to meet other process needs such as cooling via absorption refrigeration systems.

The efficiency equations are derived by taking the ratio of the desired output to the required input and are as follows:

Heat rate from diesel fuel is given by

$$\dot{Q}_{\text{H}} = \dot{V}_{\text{f}} H_{\text{v}} \quad (5)$$

The heating value used in this paper reflects a lower heating value since the exhaust gas temperatures were about 400 °C, and condensation in the exhaust was not found.

Electrical efficiency is given as

$$\eta_{\text{el}} = \frac{\dot{W}_{\text{el}}}{\dot{Q}_{\text{H}}} \quad (6)$$

Cogeneration efficiency is given as

$$\eta_{\text{cogen}} = \frac{\dot{W}_{\text{el}} + \dot{Q}_{\text{JW}}}{\dot{Q}_{\text{H}}} \quad (7)$$

Mass flow rate of jacket water (nanofluid) is calculated as follows:

$$\dot{m}_{\text{JW}} = \rho_{\text{nf}} \dot{V}_{\text{JW}} \quad (8)$$

Density of nanofluids is given as

$$\rho_{\text{nf}} = (1-\phi)\rho_{\text{f}} + \phi\rho_{\text{s}} \quad (9)$$

Heat transfer by jacket water $\dot{Q}_{JW}$ and shop water $\dot{Q}_{SW}$ are given by

$$\dot{Q}_{JW} = \dot{m}_{JW} C_{pJW} (T_{JW\text{-}out} - T_{JW\text{-}in}) \quad (10)$$

$$\dot{Q}_{SW} = \dot{m}_{SW} C_{pSW} (T_{SW\text{-}out} - T_{SW\text{-}in}) \quad (11)$$

The shop water collected the heat from the jacket water through a shell and tube heat exchanger.

7. Experimental description of DEG

The test apparatus consisted of a 45 kW generator set composed of a Mitsubishi diesel engine coupled with a Stamford generator unit (Fig. 6). This is an inline-four cylinder diesel engine with turbocharger and liquid cooling. The generator set was connected to an AC system with a 3 phase, 4 wire system, with a power factor $\geqslant 0.80$. A shell and tube heat exchanger was used to cool the jacket water and the electrical loading was provided by a set of Avtron resistor load banks. A data logger was connected such that the volumetric flow rates of the jacket water and the cooling water supply (shop water) were recorded (measured via turbine flow meters). Temperatures of both jacket and shop water inlets and outlets were recorded using type-T thermocouples, as well as the exhaust gas temperature using a type-K thermocouple. Fuel consumption was logged as well via a standing reservoir style tank with a balanced series of load cells that transduce the current tank fluid mass into a volumetric measurement. The readings were taken and stored in a data logger in 5-s intervals.

The Al_2O_3 nanofluid was obtained from the manufacturer Alfa Aesar as 50% in water colloidal dispersion. Subsequently different proportions of 50:50 EG/W were added to prepare nanofluid samples of 2%, 4% and 6% particle volume concentrations. The average particle size was 45 nm and the density was 3.6 g/cm^3 reported by the manufacturer. The specific heat of the nanoparticles is 765 J/kg K.

Fig. 7 shows the electrical output of the generator versus time. For the first 5 min, the generator was running in idling condition i.e. no electrical load was applied. When there was no electrical load, a small parasitic load for running the circulating pump was observed. In 5-min intervals,

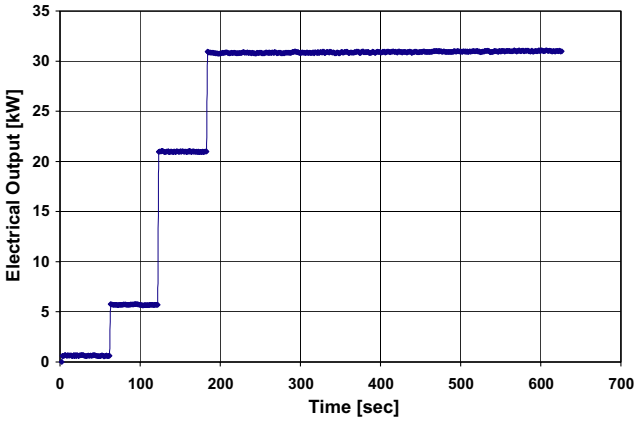

Fig. 7. Loading profile on the diesel engine. Electrical load (kW) versus time (s) when 2% Al_2O_3 nanofluid was circulating in the jacket.

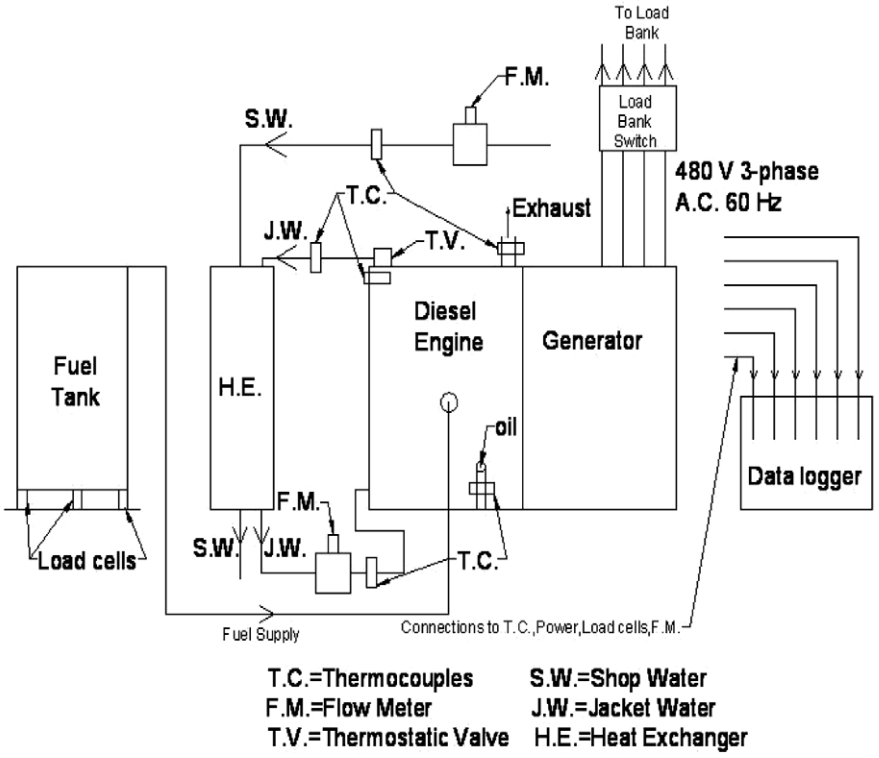

Fig. 6. Experimental setup to measure cogeneration efficiency for diesel electric generator.

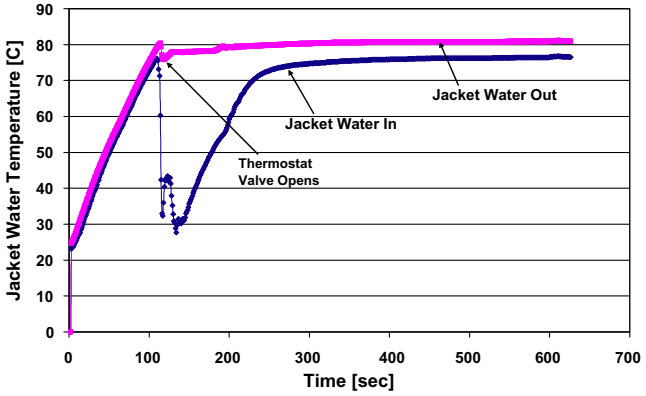

Fig. 8. Temperatures of "jacket water in" to the engine and "jacket water out" of the engine versus engine running time. In this case the jacket water was 2% Al_2O_3 nanofluid.

the electrical load was increased to 5 kW, 20 kW and finally to 30 kW. The same procedure was followed for all concentrations of Al_2O_3 nanofluids tested. We investigated the performance of nanofluids at 30 kW, when a steady state condition for jacket water flow rate and temperatures were reached.

It was observed from Fig. 8, when the engine started, the jacket water temperature was less than the set thermostatic valve temperature of 80 °C. Hence, up to 2 min (120 s) the temperature of jacket water kept on increasing. As soon as the jacket water outlet temperature reached 80 °C, the thermostatic valve opened and jacket water started circulating. There is a sudden decrease in jacket water inlet temperature as the cold fluid sitting in the radiator started flowing (see Fig. 8).

Fig. 9 displays the flow rate for shop water and jacket water (nanofluid). The shop water flow rate was kept constant around 4.5 GPM (2.84E−04 m^3/s). From Fig. 9, we can see that jacket water flow rate starts around 540 s when the flow rate is very small; the flow meter is unable to pick up small signal. But once the flow reaches around 3 GPM (1.89E−04 m^3/s) at 900 s, it picks up the signal continuously. After 2700 s the jacket water flow rate remains constant hence forth.

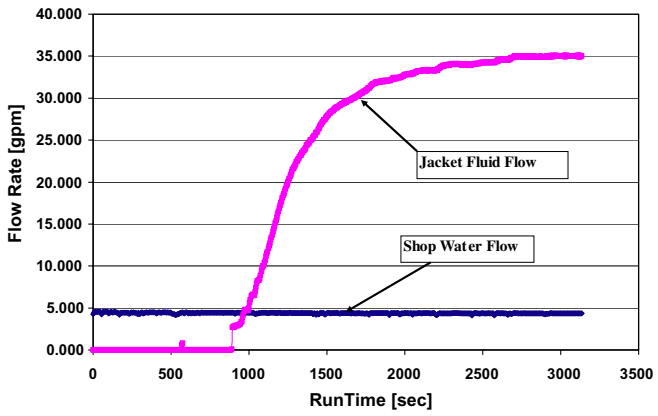

Fig. 9. Shop water and jacket fluid (4% Al_2O_3) flow rates versus time.

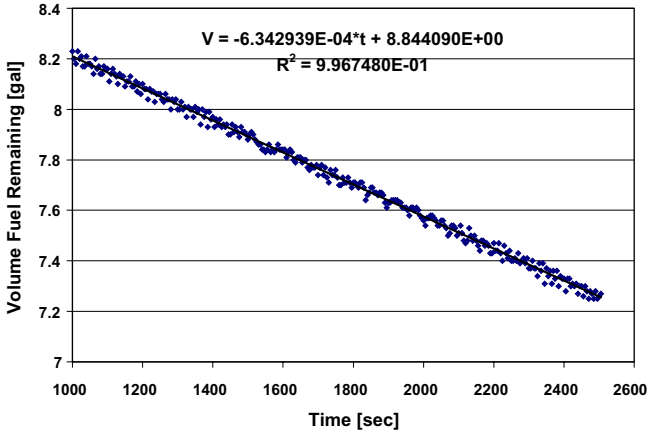

Fig. 10. Measurement of diesel fuel volume remaining in the tank versus time at constant electric load of 30 kW with 6% Al_2O_3 nanofluid as jacket coolant.

The volumetric flow rate of fuel is calculated by measuring the weight of the fuel tank using three load cells. The weight is then converted into gallons using fuel density at room temperature. Fig. 10 displays the fuel (in gallons) remaining in the tank over a period of time when the engine was running at 30 kW. The slope of this graph represents the volumetric flow rate of the fuel consumed.

Knowing the flow rate of jacket water as well as the temperatures, and the specific heat of nanofluid measured from experiment, the jacket water heat rate $\dot{Q}_{JW}$ is calculated from Eq. (10). Then the cogeneration efficiency is calculated from Eq. (4). The cogeneration efficiency with various concentrations of Al_2O_3 nanofluid is shown in Fig. 11. From this experimental study, it is observed that with increased Al_2O_3 nanoparticle concentration, the diesel engine cogeneration efficiency decreased. This is mainly attributed to a decrease in the specific heat associated with an increase in Al_2O_3 nanoparticle concentration. As a typical value, the cogeneration efficiency of EG/W mixture of 79.1%, dropped to 76.11% with 6% Al_2O_3 nanofluid.

Similarly, the cogeneration efficiency of the DEG is calculated considering the shop water heat rate and is pre-

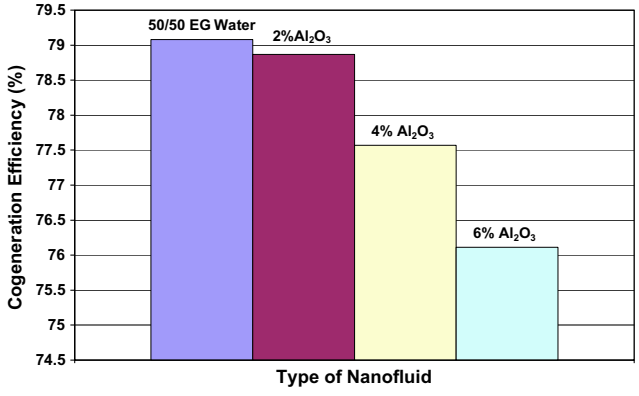

Fig. 11. Cogeneration efficiency of DEG with various concentrations of Al_2O_3 nanofluid considering jacket water heat recovery.

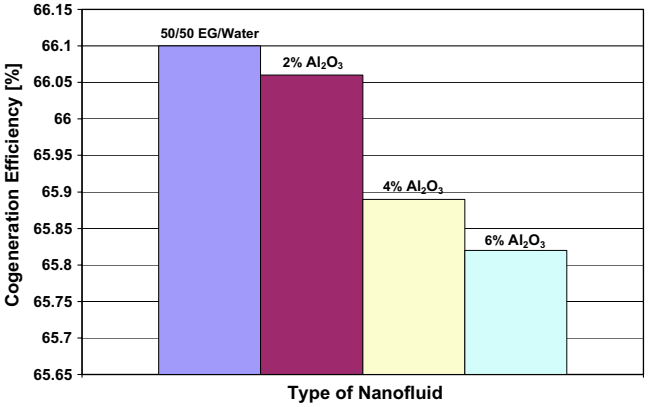

Fig. 12. Cogeneration efficiency of DEG with various concentrations of Al_2O_3 nanofluid considering shop water heat recovery.

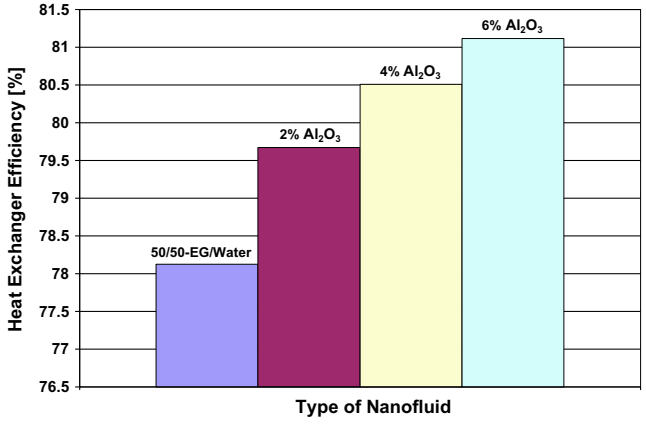

Fig. 13. Heat exchanger efficiency of the heat recovery system with various concentrations of Al_2O_3 nanofluid.

sented in Fig. 12. The results also showed that by applying nanofluids, the cogeneration efficiency decreased. As a typical value, the cogeneration efficiency decreased from 66.1% with EG/W mixture to 65.82% with 6% Al_2O_3 nanofluid.

The efficiency of the waste heat recovery heat exchanger, defined as $\dot{Q}_{SW}/\dot{Q}_{JW}$, as a function of volumetric concentration of Al_2O_3 nanofluid is shown in Fig. 13. Nanofluids flow outside the tubes and shop water flows inside the tubes in a shell and tube counter flow heat exchanger connected to the diesel engine. It is evident from Fig. 13 that with nanofluids, the heat exchanger efficiency increased. This is due to the higher heat transfer coefficient of nanofluids compared to the base fluid. For example the heat exchanger efficiency with ethylene glycol–water mixture of 78.1% increased to 81.11% for 6% Al_2O_3 nanofluid.

8. Conclusions

1. The specific heat of nanofluids decreases as nanoparticle concentration increases. The specific heat of nanofluids increases with temperature.
2. The heating time for nanofluids decreases as nanoparticles concentration in the base fluid increases. However, when the heat rate is quite large, the time difference for heating is very minimal.
3. The cogeneration efficiency of diesel generator decreases as nanoparticle concentration increases because the specific heat decreases as particle concentration increases.
4. Heat exchanger efficiency increases as particle concentration increases because of the higher heat transfer coefficients of nanofluids.
5. The future research should focus on measuring the thermophysical properties of different nanofluids as a function of temperature and concentration. Using the correlations developed new designs can be explored for heat exchangers to take the advantage of superior properties of nanofluids.

Acknowledgements

Financial assistance from the Arctic Region Supercomputing Center (ARSC) and the Dean of the Graduate School at University of Alaska Fairbanks is gratefully acknowledged.

References

[1] J.A. Phillpot, S.U.S. Choi, P.K. Keblinski, Thermal transport in nanofluids, Annual Review of Material Research 34 (2004) 219–246.
[2] S.U.S. Choi, Z.G. Zhang, P.K. Keblinski, Nanofluids, Encyclopedia of Nanoscience and Nanotechnology, vol. 6, American Scientific Publishers, 2004, pp. 757–773.
[3] M.J. Kao, H. Tsung, H.M. Lin, The friction of vehicle brake tandem master cylinder, Journal of Physics: Conference Series 48 (2006) 663–666.
[4] S.U.S. Choi, W. Yu, J.R. Hull, Z.G. Zhang, F.E. Lockwood, Nanofluids for Vehicle Thermal Management, Society of Automotive Engineers 2001-01-1706, 2001, pp. 139–144.
[5] Q. Li, X. Yimin, Convective heat transfer and flow characteristics of Cu–water nanofluid, Science in China (Series E) 45 (4) (2002) 408–416.
[6] S. Lee, S.U.S. Choi, Application of metallic nanoparticle suspensions in advanced cooling systems, Recent Advances in Solids/Structure and Application of Metallic Materials, ASME PVP-Vol. 342/MD-Vol. 72, 1996, pp. 227–234.
[7] Y. Yang, Z.G. Zhang, E.A. Grulke, W.B. Anderson, G. Wu, Heat transfer properties of nanoparticle-in-fluid dispersions (nanofluids) in laminar flow, International Journal of Heat and Mass Transfer 48 (2005) 1107–1116.
[8] D. Wen, Y. Ding, Experimental investigation into convective heat transfer of nanofluids at the entrance region under laminar flow conditions, International Journal of Heat and Mass Transfer 48 (2004) 5181–5188.
[9] Y. Ding, H. Alias, D. Wen, R. Williams, Heat transfer of aqueous suspensions of carbon nanotubes (CNT nanofluids), International Journal of Heat and Mass Transfer 49 (2006) 240–250.
[10] ASHRAE Handbook Fundamentals, American Society of Heating, Refrigerating and Air-Conditioning Engineers Inc., Atlanta, 2005.
[11] B.C. Pak, Y.I. Cho, Hydrodynamic and heat transfer study of dispersed fluids with submicron metallic oxide particles, Experimental Heat Transfer 11 (1998) 151–170.
[12] J. Buongiorno, Convective transport in nanofluids, ASME Journal of Heat Transfer 128 (2006) 240–250.

[13] Y. Xuan, Q. Li, Investigation on convective heat transfer and flow features of nanofluids, ASME Journal of Heat Transfer 125 (2003) 151–155.
[14] R.B. Mansour, N. Galanis, C.T. Nguyen, Effect of uncertainties in physical properties on forced convection heat transfer with nanofluids, Applied Thermal Engineering 27 (2007) 240–249.
[15] S.J. Palm, G. Roy, C.T. Nguyen, Heat transfer enhancement with the use of nanofluids in radial flow cooling systems considering temperature dependent properties, Applied Thermal Engineering 26 (2006) 2209–2218.
[16] S.E.B. Maiga, J. Palm, C.T. Nguyen, G. Roy, N. Galanis, Heat transfer enhancement by using nanofluids in forced convection flows, International Journal of Heat and Fluid Flow 26 (2005) 530–546.
[17] Z.S. Heris, S.Gh. Etemad, M.N. Esfahany, Experimental investigation of oxide nanofluids laminar flow convection heat transfer, International Communications in Heat and Mass Transfer 33 (2006) 529–535.
[18] Z.S. Heris, M.N. Esfahany, S.Gh. Etemad, Experimental investigation of convective heat transfer of Al_2O_3/water nanofluid in circular tube, International Journal of Heat and Fluid Flow 28 (2007) 203–210.